Spin-Lattice Interactions Mediated by Magnetic Field

J. Cao,[1,*] L. I. Vergara,[1] J. L. Musfeldt,[1] A. P. Litvinchuk,[2] Y. J. Wang,[3] S. Park,[4] and S.-W. Cheong[4]

[1]*Department of Chemistry, University of Tennessee, Knoxville, Tennessee 37996, USA*

[2]*Texas Center for Superconductivity and Department of Physics, University of Houston, Houston, Texas 77204, USA*

[3]*National High Magnetic Field Laboratory, Florida State University, Tallahassee, Florida 32310, USA*

[4]*Rutgers Center for Emergent Materials and Department of Physics and Astronomy, Rutgers University, Piscataway, New Jersey 08854, USA*

(Received 13 February 2008; published 1 May 2008)

Application of a magnetic field offers an incisive opportunity to tune competing interactions in complex materials. Here we probe field-induced changes in the local structure of $DyMn_2O_5$ by using magneto-infrared spectroscopy. The high tunability of the dielectric constant and ferroelectric polarization with field is well documented in the literature, but the lattice response on the microscopic level remains unknown. In this work, we reveal the dynamic nature of the local structural response to field and analyze it in terms of calculated mode displacements and local lattice distortions.

DOI: 10.1103/PhysRevLett.100.177205 PACS numbers: 75.80.+q, 77.80.−e, 78.20.Ls, 78.30.−j

Strongly correlated oxides derive many of their most interesting physical properties from the interplay between spin, lattice, charge, and orbital degrees of freedom. Because these interactions are so strong, complex oxides are on the ''knife's edge,'' straddling several unique regions in pressure-temperature-field space. The delicacy of this interplay makes these materials sensitive to both chemical and physical tuning. Although the overall role of the lattice is commonly acknowledged, little is known about the effect of a high magnetic field on local structure. In fact, it has generally been assumed that the lattice is rigid, with potential coupling limited by the different energy scales of magnetic and vibrational processes. Recent investments in new facilities and experiments on a wide variety of materials are, however, starting to yield a different consensus. Magnetostriction measurements and work on shape-memory materials currently provide the strongest evidence for a flexible crystalline lattice [1–8]. A few examples of magnetic field-dependent phonons are also starting to emerge, although the effects are generally small [9–12]. Materials with strong spin-phonon coupling (such as the multiferroics) offer a way to investigate potentially much larger effects.

We focused our search for sizable magnetoelastic coupling on geometrically frustrated $DyMn_2O_5$ [7,13–16]. This system displays a rich magnetic field-temperature phase diagram, with a cascade of magnetic transitions and a series of magnetic phases, the critical fields for which depend on the direction of the applied field [7,17]. Magnetostriction, thermal expansion, heat capacity, and dielectric constant measurements point toward the importance of spin-lattice coupling [7,14,18,19]. Although these measurements demonstrate changes in average structure, unit cell lattice constants, and bulk phonon contributions, they do not provide specific information on the most important local lattice displacements (i.e., bond length and angle changes) and how they differ in various magnetic states. In order to elucidate the effect of a high magnetic field on phonon modes in a material with strong spin-lattice interactions, we investigated the infrared spectral response of multiferroic $DyMn_2O_5$ as a function of temperature and magnetic field. In addition to large coupling constants and anomalous vibrational frequency shifts at several magnetic ordering temperatures (reported elsewhere), the majority of vibrational modes are sensitive to the magnetic field, indicating that the applied field modifies interionic interactions and local structure by distorting the quasioctahedral and pyramidal building block units, both locally and with respect to the Dy^{3+} centers. That spin-lattice interactions can be mediated by an applied magnetic field has important consequences for the design of functional oxides, where many exotic properties derive from a flexible lattice and strong spin-lattice-charge mixing rather than a rigid lattice and separation of the different degrees of freedom.

Single crystals of $DyMn_2O_5$ were grown by using B_2O_3-PbO-PbF_2 flux in a Pt crucible and characterized by magnetization, polarization, and x-ray diffraction. Small pieces were mixed with paraffin or KCl powder to form isotropic pellets for unpolarized transmittance measurements in the far and the middle infrared regime, respectively. Infrared transmittance measurements were performed using a series of Fourier transform infrared spectrometers, equipped with cryostats and a superconducting magnet. The absorption coefficient was calculated as $\alpha = -\frac{1}{hd}\ln T$, where h is the loading, d is the thickness, and T is the transmittance. To emphasize changes with magnetic field, we calculated the absorption difference spectra $[\alpha(H)\text{-}\alpha(0\ \mathrm{T})]/\alpha(0\ \mathrm{T})$. Lattice dynamical calculations were performed within the shell model with the general utility lattice program [20] and the crystallographic data reported in Ref. [21].

Figure 1(a) displays the 4.2 K absorption spectrum of $DyMn_2O_5$. The observed peaks are assigned via compari-

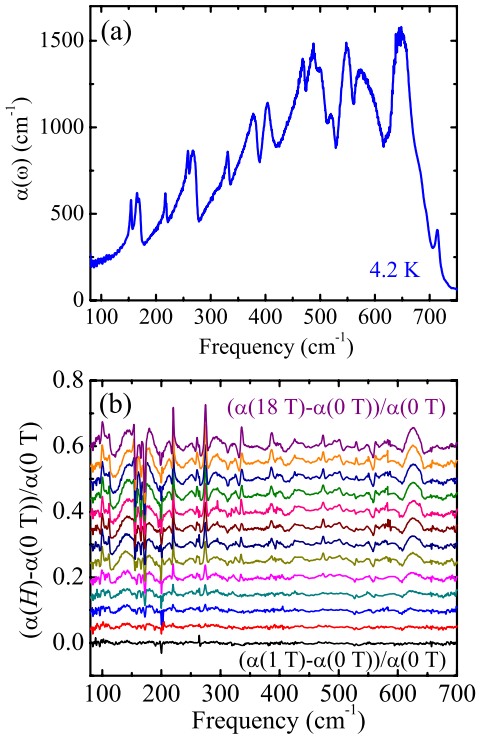

FIG. 1 (color online). (a) Absolute absorption spectrum of $DyMn_2O_5$ at 4.2 K. (b) Absorption difference spectra $[\alpha(H)\text{-}\alpha(0\ \mathrm{T})]/\alpha(0\ \mathrm{T})$ at 4.2 K for $H = 1$, 2, 3, 4, 5, 7, 8, 9, 10, 11, 13, 15, and 18 T. The curves are offset by 0.05 for clarity.

son with our lattice dynamics calculations and are in excellent agreement with results reported in Ref. [22]. The modes predicted to be between 283 and 762 cm^{-1} are due to Mn-O stretching and bending motions of the distorted octahedra and square pyramids. The lower energy features, calculated to be between 95 and 245 cm^{-1}, are mainly due to the relative motion of Mn-containing polyhedra and Dy^{3+} ions. Group theory predicts 36 infrared active vibrational modes in the paraelectric phase of $DyMn_2O_5$ at the Γ point $[\Gamma_{\mathrm{IR}} = 14B_{3u}(E \parallel a) + 14B_{2u}(E \parallel b) + 8B_{1u}(E \parallel c)]$. With the exception of mode softening between $T^* = 60$ K and T_N and small frequency shifts through the cascade of magnetic transitions, the spectrum just above T_{N1} is nearly identical to that at 4.2 K, indicating that atomic displacements that lower the structural symmetry to the noncentrosymmetric group are very small [22]. The experimental spectrum may also contain rare-earth-metal crystal-field excitations [23–25].

Figure 1(b) displays the magnetoinfrared absorption difference spectra of $DyMn_2O_5$ at 4.2 K. The majority of phonon modes display rich and surprisingly strong field dependence. Many changes are on the order of ~10% at 18 T and appear with complex derivativelike structure indicative of frequency shifts. Below, we discuss three different mode clusters as examples of the striking magnetoinfrared effects observed in $DyMn_2O_5$. These features (between 600–700, 200–300, and 140–180 cm^{-1}) were selected because they provide the best opportunity to elucidate the magnetoelastic coupling mechanism.

The broad peak and smaller dips near 630 cm^{-1} that develop in the absorption difference spectra with increasing magnetic field [Fig. 1(b)] are in the region of several calculated phonons. Although these features do not display the largest field dependence (relative changes of ~5%–6% at 18 T), they are attractive because the displacement patterns are so simple. The calculated 617 cm^{-1} mode involves relative axial or equatorial oxygen motion in the MnO_6 octahedra. The calculated 626 cm^{-1} mode arises from Mn-O stretching motion within the equatorial plane of the MnO_6 octahedra and Mn-O stretching motion in the axial direction of the MnO_5 square pyramids. The 655 cm^{-1} mode is c-polarized, involving relative motion of oxygen centers in the MnO_6 octahedra. These and other spectral features between 300 and 700 cm^{-1} can be attributed to Mn-O motion in the quasioctahedral and pyramidal building block units.

Figure 2(a) displays a close-up view of the absolute absorption and absorption difference spectra of $DyMn_2O_5$ between 600 and 700 cm^{-1}. The field-induced spectral changes are quite broad and occur gradually with the applied field. In the absolute absorption spectrum [inset, Fig. 2(a)], these changes correspond to a redistribution of oscillator strength that makes this cluster of phonons less well-defined at 18 T. In other words, intensity is lost at the peak (near 650 cm^{-1}) and recovered on the leading

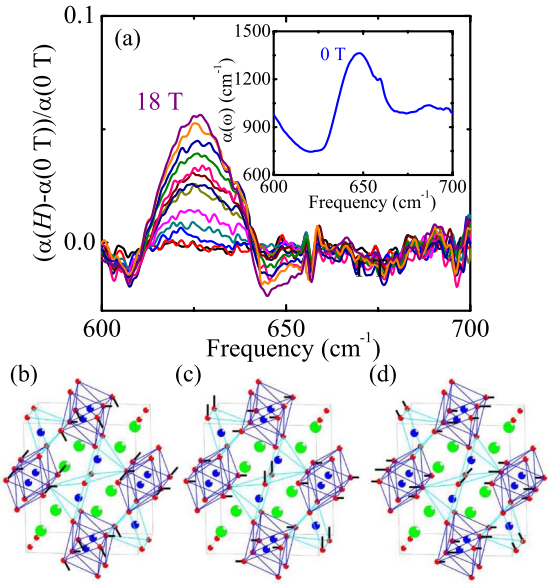

FIG. 2 (color online). (a) Main panel: Absorption difference spectra $[\alpha(H)\text{-}\alpha(0\ \mathrm{T})]/\alpha(0\ \mathrm{T})$ at 4.2 K. Inset: Close-up view of the 4.2 K absolute absorption spectrum of $DyMn_2O_5$ in zero magnetic field. (b)–(d) Representative displacement patterns of calculated 617, 626, and 728 cm^{-1} modes, respectively, corresponding to observed spectral features between 610 and 680 cm^{-1}.

edge of the absorption band near 625 cm^{-1}. No changes in peak position were observed within our sensitivity. The field-induced redistribution of oscillator strength demonstrates that the magnetic field is influencing the transition matrix elements. As discussed below, this probably occurs due to a change in local structure and consequent modification of interionic interactions.

Correlations between magnetic order and the lattice have attracted attention in rare-earth-metal manganites and other complex oxides [10,26,27]. In $DyMn_2O_5$, longitudinal magnetostriction studies are particularly useful, with changes along the three crystallographic directions on the order of 10^{-4} [7]. Importantly, $\Delta a/a$ increases with the applied magnetic field, whereas $\Delta b/b$ and $\Delta c/c$ show an overall decrease. Examination of the crystal structure shows that a is the softest direction that is, on average, perpendicular to the axial bonds of the MnO_6 octahedra. b is, on average, parallel to the axial bonds. The a-axis expansion and b-axis contraction point toward a field-induced "squashing" of the octahedra. This scenario is consistent with the observed magnetoinfrared spectra and the suggestion that an applied magnetic field deforms the local structure of the octahedral and square pyramidal building blocks. Local structure changes modify orbital overlap ($t = \int \phi_i H \phi_j d\tau$ between sites i and j) which affects the Mn-O-Mn superexchange interaction as $J \sim t^2/U$.

Large coupling constants (λ's) are also observed for several of the bending modes. Those between 200 and 300 cm^{-1} change substantially in magnetic field [Fig. 1(b)]. The features near 220 cm^{-1} in the absorption difference spectra are assigned to calculated phonons at 208 and 231 cm^{-1}. The 208 cm^{-1} phonon is due to the relative motion between Dy^{3+} ions and equatorial oxygens in the Mn octahedra, and the 231 cm^{-1} feature derives from the relative motion of oxygen centers. The peak at 270 cm^{-1} in the absorption difference response is assigned to the calculated phonon at 283 cm^{-1}. The displacement pattern of this mode mainly involves torsional and twisting motions of the MnO_6 octahedra along a (the equatorial plane direction).

Figure 3 displays a close-up view of the absolute absorption and absorption difference spectra of $DyMn_2O_5$ between 200 and 300 cm^{-1}. The absorption difference data show features with $\geq 10\%$ deviation from zero at 18 T and derivativelike line shapes that are indicative of small field-induced frequency shifts. By calculating the absolute absorption, we see that the trailing edges of the 217 and 267 cm^{-1} spectral peaks blueshift in the magnetic field. The sensitivity of the 217 cm^{-1} feature to both applied field and temperature (across T_{N1} and T_{C2}) is consistent with a magnetoelastic coupling mechanism involving (i) the displacement of Dy centers with respect to the equatorial O plane in the octahedra along the b direction and (ii) local twisting and squashing of the MnO_6 octahedra favoring the soft a direction. These distortions modify Mn-O-Mn exchange interactions.

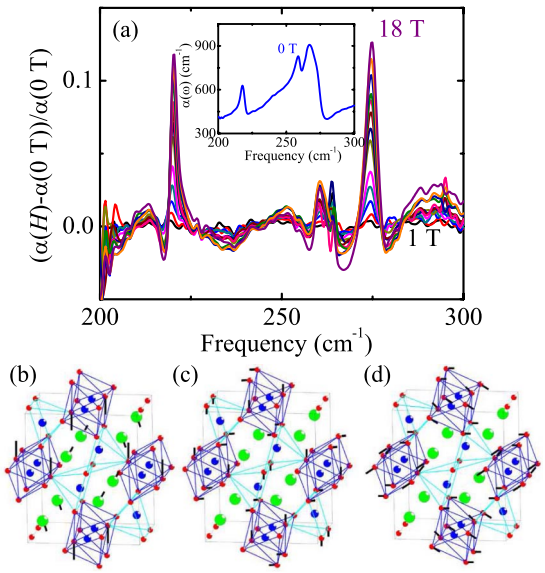

FIG. 3 (color online). (a) Main panel: Absorption difference spectra $[\alpha(H)\text{-}\alpha(0\ T)]/\alpha(0\ T)$ at 4.2 K. Inset: Close-up view of the 4.2 K absolute absorption spectra of $DyMn_2O_5$ in zero magnetic field. (b)–(d) Representative displacement patterns of calculated 208, 231, and 283 cm^{-1} modes, respectively, corresponding to observed spectral features between 200 and 300 cm^{-1}.

The peaks between 140 and 180 cm^{-1} in the infrared absorption spectrum of $DyMn_2O_5$ [Fig. 1(a)] are assigned as a superposition of predicted 170–189 cm^{-1} phonons and Dy^{3+} crystal-field excitations [23–25]. Because of this superposition, the field-induced spectral changes are more complicated, with both magnetoelastic and crystal-field effects. Figures 4(a) and 4(b) display a close-up view of the absolute absorption and absorption difference spectra between 140 and 180 cm^{-1}, respectively. This spectral range exhibits a number of lines that are much sharper than those at higher frequencies. The relatively narrow (3–5 cm^{-1}) features may be due to intermultiplet transitions of the ${}^6H_{15/2}$ ground state of Dy^{3+}, which splits into 8 levels in the local field below cubic symmetry. Detailed measurements on single crystals in polarized light will be able to separate these effects from magnetoelastic contributions.

In addition to large λ's that facilitate field-induced modification of local structure, an applied magnetic field also drives the system through a series of magnetic ground states [7,17]. This cascade of field-induced transitions has the potential to be associated with changes in the lattice. To test this idea, we plotted peak positions and integrated oscillator strengths of lines in the 140–180 cm^{-1} range as a function of applied field [Figs. 4(c) and 4(d)]. We find that the peak positions and integrated area are sensitive to the ferroelectric 3 to ferroelectric 2 transition ($H \parallel b$) near

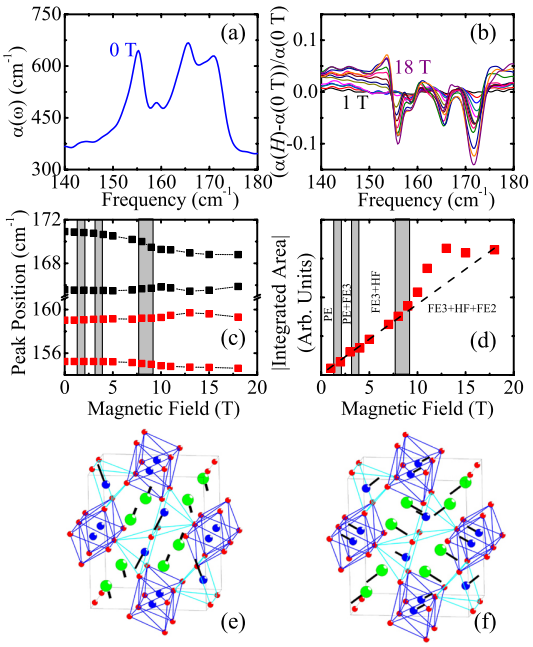

FIG. 4 (color online). (a) Close-up view of the 4.2 K absolute absorption spectra of $DyMn_2O_5$ at 0 T. (b) Absorption difference spectra $[\alpha(H)\text{-}\alpha(0\ \mathrm{T})]/\alpha(0\ \mathrm{T})$ at 4.2 K. (c) Magnetic field dependence of the peak positions. (d) Absolute value of the integrated area of the absorption difference spectra in the 140–180 cm^{-1} range. The gray vertical lines in (c) and (d) denote the critical fields [7], although the response is averaged for an isotropic sample. Error bars on the points in (c) and (d) are on the order of the symbol size, and the dashed line in (d) is a guide to the eye. (e)–(f) Representative displacement patterns of calculated 170 and 176 cm^{-1} modes, respectively.

8.5 T, providing additional evidence for strong spin-lattice coupling in this system and the role of relative MnO_6 and MnO_5 polyhedra motion with respect to the Dy^{3+} centers. The Dy^{3+} displacement modes between 95 and 110 cm^{-1} [Fig. 1(b)] are weakly sensitive to the $H \parallel c$ transition near ~4 T (paraelectric phase to high field phase) as well.

The static magnetodielectric effect in $DyMn_2O_5$ is a prominent example of the intriguing interplay between spin and lattice degrees of freedom made manifest in the bulk properties [13]. The dispersive contrast ($\geq 100\%$ below 25 K at 7 T) gains its strength from nearby dipole-allowed excitations. The electromagnon [28] and crystal-field excitations [24] have both been shown to contribute to this response. The magnetic field-dependent phonons identified here provide additional candidates of appropriate energy and symmetry, although the relative importance of any particular excitation to the static magnetodielectric contrast decreases with increasing frequency. The data in Fig. 1(b) demonstrate magnetoelectric coupling at ac frequencies, complementing and extending the aforementioned static results.

The observation that local structure, as measured by the infrared vibrational properties, is sensitive to the magnetic state in $DyMn_2O_5$ has important consequences for the design of functional oxides. In this system, it explains the underlying phonon contribution to many of the observed bulk property trends, detailing which phonons are involved and connecting the important features to their displacement patterns. Such phenomena are not only important for multiferroic oxides but for all correlated oxides, where many exotic properties derive from spin-lattice-charge coupling rather than a rigid lattice and separation of the different degrees of freedom.

This work is supported by the DOE (UT, NHMFL), the NSF (Rutgers, NHMFL), the State of Texas (UH), and the State of Florida (NHMFL). We thank C. J. Fennie, B. Harris, B. Lorenz, J. Lynn, M. Mostovoy, and I. Sergienko for useful discussions.

*Present address: Materials Sciences Division, Lawrence Berkeley National Laboratory, Berkeley, CA 94720, USA, and Department of Materials Science and Engineering, University of California, Berkeley, CA 94720, USA.

[1] T. Kimura *et al.*, Phys. Rev. Lett. **81**, 5920 (1998).
[2] B. García-Landa *et al.*, Phys. Rev. Lett. **84**, 995 (2000).
[3] A. N. Lavror, S. Komiya, and Y. Ando, Nature (London) **418**, 385 (2002).
[4] S. E. Russek *et al.*, J. Appl. Phys. **91**, 8659 (2002).
[5] H. Yamaguchi *et al.*, Europhys. Lett. **72**, 479 (2005).
[6] V. S. Zapf *et al.*, J. Appl. Phys. **101**, 09E106 (2007).
[7] C. R. dela Cruz *et al.*, Phys. Rev. B **74**, 180402(R) (2006).
[8] Y. Boonyongmaneerat *et al.*, Phys. Rev. Lett. **99**, 247201 (2007).
[9] T. Ruf *et al.*, Phys. Rev. B **38**, 11 985 (1988).
[10] A. B. Sushkov *et al.*, Phys. Rev. B **66**, 144430 (2002).
[11] R. Wesolowski *et al.*, Phys. Rev. B **71**, 214514 (2005).
[12] M. Rini *et al.*, Nature (London) **449**, 72 (2007).
[13] N. Hur *et al.*, Phys. Rev. Lett. **93**, 107207 (2004).
[14] C. R. dela Cruz *et al.*, Phys. Rev. B **73**, 100406(R) (2006).
[15] G. R. Blake *et al.*, Phys. Rev. B **71**, 214402 (2005).
[16] B. Lorenz, Y. Wang, and C. W. Chu, Phys. Rev. B **76**, 104405 (2007).
[17] W. Ratcliff II *et al.*, Phys. Rev. B **72**, 060407(R) (2005).
[18] S.-W. Cheong and M. Mostovoy, Nat. Mater. **6**, 13 (2007).
[19] M. Mostovoy, Phys. Rev. Lett. **96**, 067601 (2006).
[20] G. D. Gale, J. Chem. Soc., Faraday Trans. **93**, 629 (1997).
[21] S. C. Abrahams and J. L. Bernstein, J. Chem. Phys. **46**, 3776 (1967).
[22] C. Wang, G.-C. Guo, and L. He, Phys. Rev. Lett. **99**, 177202 (2007).
[23] P. Allenspach, A. Furrer, and F. Hulliger, Phys. Rev. B **39**, 2226 (1989).
[24] A. A. Sirenko *et al.*, arXiv/cond-mat/0703255.
[25] M. Divis *et al.*, J. Alloys Compd. **451**, 662 (2008).
[26] I. A. Sergienko, C. Şen, and E. Dagotto, Phys. Rev. Lett. **97**, 227204 (2006).
[27] A. Garg, Phys. Rev. Lett. **81**, 1513 (1998).
[28] A. B. Sushkov *et al.*, Phys. Rev. Lett. **98**, 027202 (2007).